

Influence of the transfer of fast charged particles – products of thermonuclear reactions – on the burning of targets

G.V. Dolgoleva, A.I. Zykova

Abstract. The nonstationary energy transfer by fast charged particles, i.e. products of thermonuclear reactions, is simulated, and the effect of this process on the compression and burning of thermonuclear targets is numerically investigated.

Keywords: laser plasma, charged particles, thermonuclear reactions, particle transfer.

1. Introduction

The limited possibilities in carrying out experiments with full-scale thermonuclear burning of targets make it necessary to resort to numerical modelling. This not only allows one to explain the results of the experiments and contributes to their understanding, but also facilitates the performance of the experiments themselves and their prediction.

The problem of the creation and transfer of charged particles arising as a result of thermonuclear reactions in a burning deuterium–tritium plasma is very important. Often the calculation of target burning is carried out in the approximation of local energy release by fast charged particles, that is, it is assumed that the particle gives its energy at the same point in the space in which it originated. However, when the excess over the target ignition threshold is small, in determining the target parameters and also in evaluating the characteristics of the laser setup necessary to accomplish the target ignition, the model must accurately reflect where and how charged particles give up their energy, i.e., it is important to calculate the nonstationary energy transfer by fast charged particles, i.e. products of thermonuclear reactions. In what follows, they will be called fast charged particles.

At first glance, it seems that taking into account the transfer of fast charged particles in the target should lead to a decrease in energy release in the region where the DT fuel (DT region) is located since part of the energy is transferred to neighbouring regions and does not participate in the burning of the target. This reduces the temperature of the DT region and the yield of thermonuclear energy. Naturally, the target gain (the ratio of the released thermonuclear energy to the energy deposited in the target) decreases. A numerical study has shown that this is not always the case. The energy trans-

ferred from the DT region is localised in the adjacent region, where the bulk density of energy and pressure (and thus the expansion of the DT region is constrained), as well as the burning time of the DT gas and the thermonuclear energy yield increase.

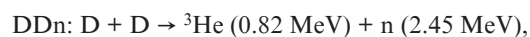
The task of studying the transfer of energy by charged thermonuclear particles in compressed laser targets is not new [1–3]. Vygovskii et al. [1] considered the deceleration of fast charged particles in an ideal plasma, paper [2] was devoted to the simulation of the energy transfer by charged thermonuclear particles in compressed laser targets with allowance for spontaneous magnetic fields, and Bel'kov et al. [3] described in detail the nonstationary mathematical model for the transfer of fast charged particles and studied the effect of this process on the burning of a specific thermonuclear target for the NIF facility.

The aim of this paper is to consider the effect of charged-particle transfer on the parameters of micro-targets used in laser and thermonuclear fusion, using examples of known targets.

2. Model of the transfer of fast charged particles

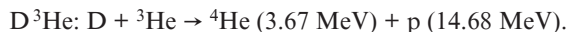
All computational experiments were carried out using a technique oriented toward numerical investigation of the physical processes taking place in a laser plasma [4]. The following processes are calculated in the programme: motion of the medium in the presence of 'detachment' of temperatures (ions and electrons), absorption of laser energy with allowance for reflection from the critical density region, heat transfer by electrons and ions with diffusion flux restrictions, spectral radiation transfer in the quasi-diffusion approximation [5] and its interaction with matter, ionisation of matter and the excitation of ions in a nonequilibrium nonstationary plasma, kinetics of thermonuclear reactions and energy transfer of by fast charged particles. The equations of state, spectral ranges of radiation, coefficients of the electron and ion thermal conductivity, electron–ion relaxation and absorption of laser energy were calculated taking into account the plasma composition [6].

Numerical simulation of a thermonuclear target takes into account four types of reactions:



G.V. Dolgoleva, A.I. Zykova Research Institute of Applied Mathematics and Mechanics, Tomsk State University, prosp. Lenina 36, str. 27, 634050 Tomsk, Russia;
e-mail: dolgg@list.ru, Arven2022@mail.ru

Received 27 March 2017; revision received 7 August 2017
Kvantovaya Elektronika 47 (12) 1166–1170 (2017)
Translated by I.A. Ulitkin



The reaction rates are taken from [7]. One more model is known for the reaction rates [8]. Differences in the results of calculations of energy release, carried out using these two models for reaction rates, are about 10% [9]. Which model is more correct is difficult to say, because a comparison with experimental data is necessary. The analysis carried out in [10], taking into account the measurements performed by Krauss et al. [11], as well as the theoretical results obtained in [11], allowed the authors of [10] to conclude that the initial data on the rates of processes [7], published in 1962, withstood the test of time over a wide range of energies.

The transfer of fast charged particles is calculated in the multigroup diffusion approximation. The equation for the transfer of fast charged particles is obtained from the kinetic equation by integrating the latter over the angle and is described in detail in [3]. It shows that the use of multigroup diffusion in the energy transfer by fast charged particles gives satisfactory accuracy in the calculations of thermonuclear burning. The difference from the results of calculations with allowance for the energy transfer by particles in the kinetic approximation is no more than 15%, i.e., the calculations are reliable.

3. Formulation of the problem and results of calculations

The effect of the particle transfer on the parameters of micro-targets used in laser and fusion synthesis was considered by us on examples of known targets [12–14]. In the calculations, we took into account all the processes described above.

For each calculation, we present a table that contains the following values: E is the energy deposited in the target, F is the energy released from the thermonuclear reactions, F_α is the energy of fast charged particles obtained by burning the target, Δ is the fraction of the energy released by charged particles from the DT regions and K is the target gain ($K = F/E$). Tables 1, 2 and 4 show the results of target calculations without taking into account the transfer of fast charged particles (upper row) and with allowance for the transfer (bottom row).

The first task is the calculation of the direct compression target [12]. The geometry of the target and the shape of the laser pulse are shown in Figs 1 and 2, respectively, and the results of this calculation are listed in Table 1. In Fig. 1, the first region is the DT gas, the second one is the DT ice, and the third one is the CH polymer.

| | DT gas | | DT ice | | CH | |
|-------------------------|--------|--------|--------|--------|----|--|
| r/cm | 0 | 0.1411 | 0.1563 | 0.1597 | | |
| $\rho/\text{g cm}^{-3}$ | 0.001 | 0.253 | 1.05 | | | |

Figure 1. Geometry of the target: r is the spatial variable; ρ is the initial density of the layers.

A laser pulse with a wavelength $\lambda = 0.35 \mu\text{m}$ is absorbed in the layers of the target with an electron density below the critical value. Unabsorbed radiation is reflected from the critical density region and is absorbed in the ‘corona’ during its backward pass.

With a local energy release from fast charged particles due to the burning of the micro-target, a thermonuclear energy of

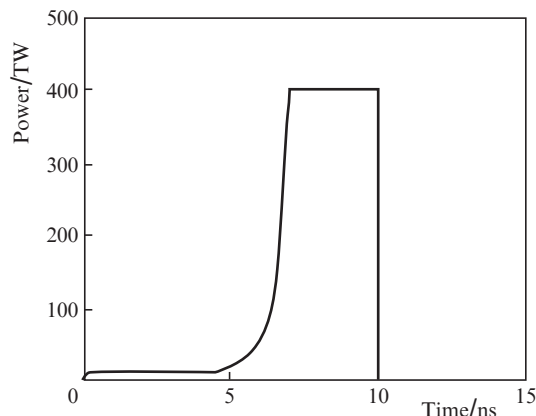


Figure 2. Shape of the laser pulse.

Table 1.

| E/MJ | F/MJ | F_α/MJ | $\Delta (\%)$ | K |
|---------------|---------------|----------------------|---------------|------|
| 1.48 | 9.84 | – | – | 6.65 |
| 1.48 | 6.2 | 6.1 | 7.3 | 4.2 |

9.84 MJ is released, and the target gain K is 6.65. In the calculation, taking into account the transfer of particles, an energy of 6.2 MJ is released, and the target gain is reduced to 4.2. An energy of 6.1 MJ is released by fast particles, with 7.3% of this energy (0.444 MJ) being transferred by particles to the region with CH, and is excluded from the process of thermonuclear burning. Consequently, when the energy transfer by fast charged particles is taken into account, the energy release as a result of thermonuclear reactions decreases, since part of the energy is removed from DT regions into the CH region and does not participate in thermonuclear reactions.

Figures 3–6 show the distributions of the target density, electron and ion temperatures and pressure as a function of radius at the time instant of a maximum energy release (for the case without the transfer of fast charged particles at 10.43 ns, for the case with their transfer at an instant of time 10.46 ns), and Fig. 7 demonstrates the value of $W = \int_{\text{DT}} \rho dr$ as a function of time. The boundary between the DT and CH regions is located at $r = 0.04 \text{ cm}$ in both calculations for the given target.

Differences in the distributions of all quantities are noticeable, but we would especially like to draw attention to the difference in ion temperatures in the two calculations, since

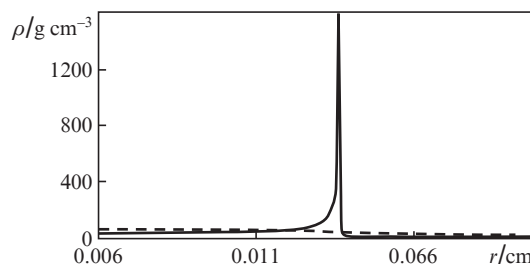


Figure 3. Radial distributions of the target density ρ . Here and in Figs 4–7, dashed curves are a calculation with allowance for the energy transfer by fast charged particles, and solid curves are calculations without taking the energy transfer into account.

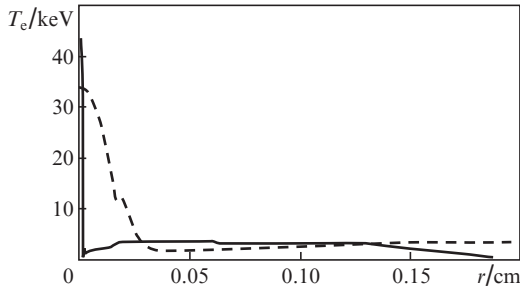


Figure 4. Radial distributions of electron temperature T_e .

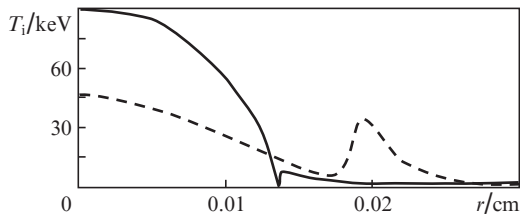


Figure 5. Radial distributions of ion temperature T_i .

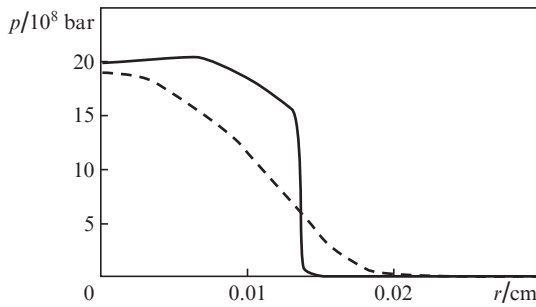


Figure 6. Radial distributions of pressure p .

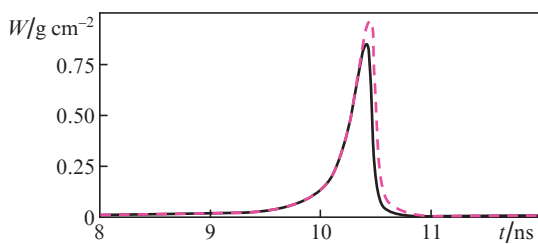


Figure 7. Time dependences of the quantity $W = \int_{DT} \rho dr$.

the reaction rates and the amount of the released thermonuclear energy depend on them.

In the second calculation, we simulate the heating and compression of a shell target made of a CH polymer filled with a DT mixture. In comparison with the previous problem, here we deal with a different geometry and a different shape of the pulse. The geometry of the target (Fig. 8) and the shape of the pulse are taken from [13].

The target is irradiated by laser radiation with a wavelength $\lambda = 0.35 \mu\text{m}$ and a pulse energy of 1 MJ. The laser pulse has a rising leading edge up to the instant of time t_1 , then a plateau in the interval $t_1 < t < t_2$ and a rapidly falling trailing edge:

| | | | | |
|-------------------------|--------|--------|--------|-----|
| | DT gas | | DT ice | CH |
| r/cm | 0 | 0.1956 | 0.1965 | 0.2 |
| $\rho/\text{g cm}^{-3}$ | | 0.0007 | 0.25 | 1 |

Figure 8. Geometry of the target.

$$\dot{E}(t) = \dot{E}_0 \begin{cases} \left(\frac{t}{t_1}\right)^2 & \text{for } t < t_1, \\ 1 & \text{for } t_1 < t < t_2, \\ \frac{t_3 - t}{t_3 - t_2} & \text{for } t_2 < t < t_3, \end{cases} \quad (1)$$

$$\dot{E}_0 = E_{\text{las}} \left(\frac{t_3 + t_2}{2} - \frac{2}{3} t_1 \right)^{-1},$$

where $t_1 = 8 \text{ ns}$; $t_2 = 10 \text{ ns}$; $t_3 = 11 \text{ ns}$; and $E_{\text{las}} = 1 \text{ MJ}$.

The calculation shows that all the laser energy E_{las} is completely absorbed in the ‘corona’ during the forward and backward passages. Table 2 shows the results of this calculation.

Table 2.

| E/MJ | F/MJ | F_d/MJ | $\Delta(\%)$ | K |
|---------------|---------------|-----------------|--------------|------|
| 1 | 2.265 | – | – | 2.26 |
| 1 | 2.543 | 2.494 | 57.9 | 2.54 |

Figures 9–12 show the distributions of the target density, electron and ion temperatures and pressure as a function of the radius at the time instant of a maximum energy release (for the case without the transfer of fast charged particles at 10.31 ns, for the case with their transfer at an instant of time 10.29 ns), and Fig. 13 demonstrates the value of W as a function of time. The boundary between the DT and CH regions corresponds to $r = 0.07 \text{ cm}$ in both calculations for the given target.

It can be seen from Figs 9–12 that for this target the maxima of the distributions of the target density, temperatures and pressures are higher in the CH region when calculations take into account the energy transfer by fast charged particles.

What explains this difference in calculation results for the first and second targets? What is more important: the geometry of the system or the shape of the laser pulse? Table 3 lists the calculation results for the second target, while maintaining its geometry, but for the same shape of the laser pulse as for the first target (top row), and also for the case when the

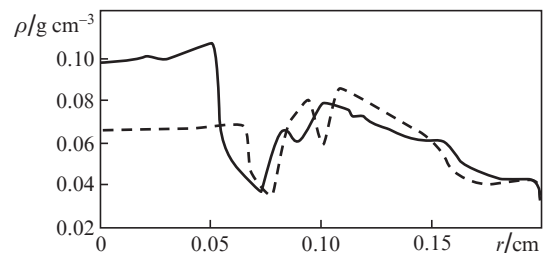


Figure 9. Radial distributions of the target density ρ . Here and in Figs 10–13, dashed curves are a calculation with allowance for the energy transfer by fast charged particles, and solid curves are calculations without taking the energy transfer into account.

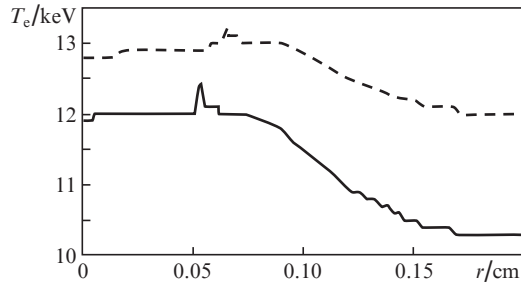
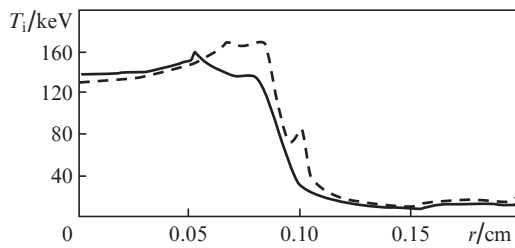
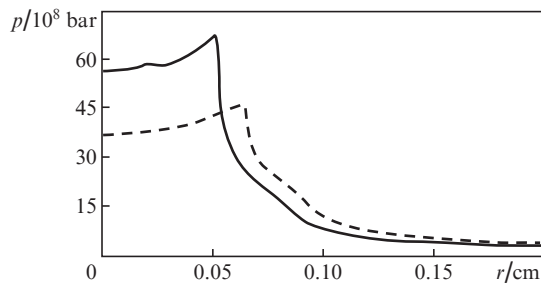
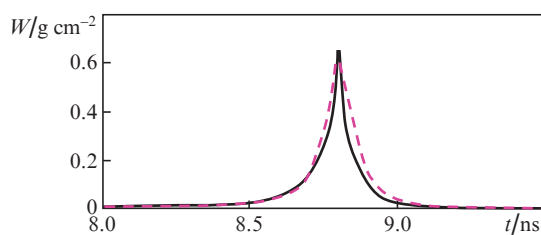

Figure 10. Radial distributions of electron temperature T_e .

Figure 11. Radial distributions of ion temperature T_i .

Figure 12. Radial distributions of pressure p .

Figure 13. Time dependences of the quantity $W = \int_{DT} \rho dr$.

Table 3.

| E/MJ | F/MJ | F_a/MJ | $\Delta(\%)$ | K |
|---------------|---------------|-----------------|--------------|------|
| 1.48 | 1.915 | 1.88 | 60 | 1.3 |
| 1 | 1.757 | 1.732 | 63 | 1.76 |

total energy of the pulse is reduced by 1.48 times, so that the deposited energy is equal to 1 MJ (bottom row), as in the first calculation for the second target. From these calculations, we can draw the following conclusion: for these targets, the energy release depends on the shape of the laser pulse rather than on the geometry of the target.

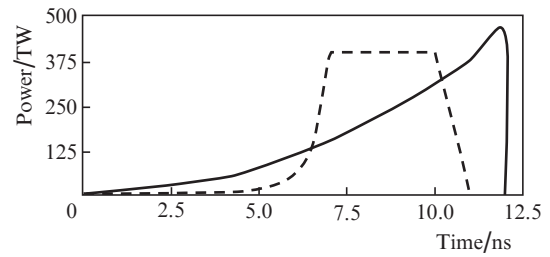

Figure 14. Shapes of laser pulses used in calculations for the first (solid curve) and second (dashed curve) targets.

Figure 14 compares the shapes of laser pulses used in calculations for the first and second targets.

The next calculation, where we study the effect of the energy transfer by fast particles on the target parameters, is the calculation of a cylindrical target for synthesis on heavy ions (Fig. 15). In this micro-target [14], the first layer is the DT layer, thin layers 2 and 4 consist of dense materials (gold) – ‘heavy’ layers, and external laser radiation is introduced into the ‘light’ layer 3 (‘perforated’ lead). The functions of the heavy layers are to suppress the expansion of the DT region and the target. The energy is deposited in layer 2 so that at the boundary of the DT region, the specified velocities and pressures necessary for its unstressed compression are provided [15].

| | DT | Au | Pb | Au | |
|-------------------------|------|------|------|------|-------|
| r/cm | 0 | 0.2 | 0.21 | 0.39 | 0.444 |
| $\rho/\text{g cm}^{-3}$ | 0.05 | 19.5 | 6 | 19.5 | |

Figure 15. Geometry of the target for synthesis on heavy ions.

To reproduce unstressed compression on the right boundary of the working DT region, the velocity and pressure in the case of an ideal gas must be represented in the form (these dependences were obtained by Stanyukovich [15])

$$u = \frac{2}{\gamma - 1} c_0 \left[1 - \left(1 - \frac{c_0}{L_0} t \right)^{\frac{\gamma-1}{\gamma+1}} \right],$$

$$p = \frac{\rho_0}{\gamma} c_0^2 \left(1 - \frac{c_0}{L_0} t \right)^{-\frac{2\gamma}{\gamma+1}} = p_0 \left(1 - \frac{c_0}{L_0} t \right)^{-\frac{2\gamma}{\gamma+1}},$$

where L_0 is the length of the compressible layer; ρ_0 and c_0 are the initial density and speed of sound, respectively; and γ is the adiabatic exponent.

The time dependence of the energy deposition for this case is given in [14], the numbering of layers from the centre beginning with the zeroth layer:

$$\frac{\partial E}{\partial t} = Q(t), \quad Q(t) = \frac{2\gamma c_0^3 G}{(\gamma - 1)^2 m_2} L_0^\alpha \left\{ - \left(1 - \xi \frac{\gamma-1}{\gamma+1} \right)^2 + \left[\frac{V_2(0)}{aL_0^\alpha} + (\gamma - 1) + 2\xi - (\gamma + 1)\xi \frac{2\gamma}{\gamma+1} \right] \frac{\xi^{-1}}{\gamma+1} \right\} \xi^{-\frac{2\gamma}{\gamma+1}} L_0^{\alpha-1},$$

$$\xi = 1 - \frac{c_0 t}{L_0} (0 \leq \xi \leq 1),$$

$$G = \frac{m_0}{\gamma}(1 - 2k_2) + \frac{2k_1}{\gamma + 1} + \frac{(\gamma + 1)m_0^2}{\gamma^2}k_3,$$

$$a = \frac{m_1 + m_2 + m_3 + \frac{\gamma + 1}{2\gamma}\rho_0 L_0^\alpha}{(\gamma - 1)\left(\frac{m_2}{2} + m_3\right)},$$

$$k_1 = m_1 + \frac{m_2}{3} + \frac{m_1 + \frac{m_2}{2}}{\left(m_3 + \frac{m_2}{2}\right)^2}\left(\frac{m_1 m_2}{3} + m_1 m_3 + \frac{m_2 m_3}{6}\right),$$

$$k_2 = -\frac{1}{\left(m_3 + \frac{m_2}{2}\right)^2}\left[\frac{m_2}{3}\left(m_3 + \frac{m_2}{4}\right) + m_1\left(m_3 + \frac{m_2}{3}\right)\right],$$

$$k_3 = -\frac{m_3 + \frac{m_2}{3}}{2\left(m_3 + \frac{m_2}{2}\right)^2}.$$

Here, m_i and $V_i(0)$ are the masses and volumes of the layers ($i = 0-3$), respectively; and α is a parameter that depends on the target geometry. The energy deposition is calculated by this formula until $Q(t) < Q^*$ (Q^* is the so-called maximum specific absorption rate, the characteristic of the laser setup), and then by the formula $\partial E/\partial t = Q^*$, until the required amount of energy is deposited (in this case, 21 MJ).

The function $Q(t)$ is shown in Fig. 16 for a specific target with $c_0 = 0.01 \text{ cm ns}^{-1}$ and $L_0 = 0.1 \text{ cm}$ and for the maximum specific absorption rate $Q^* = 60 \text{ TW g}^{-1}$. The length in the above formulas is measured in cm, the time in ns, and $Q(t)$ in TW g^{-1} . Quantitatively, the values of $Q(t)$ differ in different calculations depending on the geometry of the target (or masses m_i), the maximum value of Q^* , the values of c_0 and L_0 , but the shape of the curves is the same (with the specific absorption rate). The results of the calculation for this target are listed in Table 4.

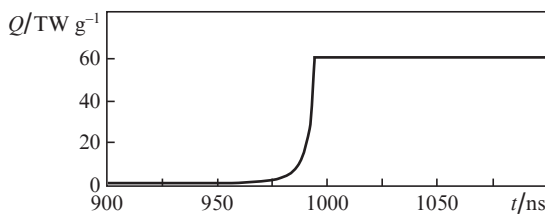


Figure 16. Dependence of Q on t .

Table 4.

| E/MJ | F/MJ | F_a/MJ | Δ (%) | K |
|---------------|---------------|-----------------|--------------|------|
| 21 | 25.6 | – | – | 1.22 |
| 21 | 27.2 | 24.67 | 17 | 1.3 |

Without taking into account the energy transfer by fast particles, the energy released amounts to 25.6 MJ, and when the transfer is taken into account, it is 27.2 MJ. At the same time, 17% (4.19 MJ) of energy is removed from the DT region by fast particles of thermonuclear reactions and is localised in the neighbouring region made of gold. Therefore, the expansion of the DT region is restrained and its burning intensifies.

Thus, in the present work, modelling is carried out on the basis of spectral diffusion equations for the transfer of fast particles that arise as a result of thermonuclear reactions. It is

shown that the transfer of fast charged particles can both reduce and increase the energy release in the DT region, depending on the shape of the laser pulse and the geometry of the target.

References

1. Vygovskii O.B., Il'yin D.A., Levkovskii A.A., Rozanov V.B., Sherman V.E. Preprint FIAN No. 72 (Moscow, 1990).
2. Konash P.V., Lebo A.I., Lebo I.G. *Mat. Model.*, **25**, 3 (2013).
3. Bel'kov S.A., Dolgoleva G.V., Ermolovich V.F. *VANT. Ser. Mat. Model. Fiz. Protsess.*, issue 1, 51 (2003).
4. Dolgoleva G.V. *VANT. Ser. Metod. Program. Chisl. Resheniya Zad. Mat. Fiz.*, issue 2 (13), 29 (1983).
5. Gol'din V.Ya., Chetverushkin B.P. Preprint IAM No. 12 (Moscow, 1970).
6. Bel'kov S.A., Dolgoleva G.V. *VANT. Ser. Mat. Model. Fiz. Protsess.*, issue 1, 59 (1992).
7. Kozlov B.N. *At. Energ.*, **12** (3), 238 (1962).
8. Basco M.M. Preprint ITEP No. 145 (Moscow, 1985).
9. Dolgoleva G.V., Zabrodina E.A. Preprint KIAM No. 68 (Moscow, 2014).
10. Imshennik V.S., Litvinova I.Yu. Preprint ITEP No. 69 (Moscow, 1990).
11. Krauss A., Becker H.W., Trautvetter H.P., Rolfs C., Brand K. *Nucl. Phys. A*, **465**, 150 (1987).
12. Bel'kov S.A., Bondarenko S.V., Vergunova G.A., et al. *JETP*, **121** (4), 686 (2015) [*Zh. Eksp. Teor. Fiz.*, **148**, (4 (10)), 781 (2015)].
13. Dolgoleva G.V., Lebo A.I., Lebo I.G. *Mat. Model.*, **28** (1), 23 (2016).
14. Dolgoleva G.V., Zabrodin A.V. *Kumulyatsiya energii v sloistyykh sistemakh i realizatsiya bezudarnogo szhatiya* (Cumulation of Energy in Layered Systems and Realization of Unstressed Compression) (Moscow: Fizmatlit, 2004).
15. Stanyukovich K.P. *Unsteady Motion of a Continuous Medium* (Oxford: Pergamon Press, 1960; Moscow: Nauka, 1971).